Kidney International, Vol. 66 (2004), pp. 91–101

Stable expression of nephrin and localization to cell-cell contacts in novel murine podocyte cell lines

Daniel Schiwek, Nicole Endlich, Lawrence Holzman, Harry Holthöfer, Wilhelm Kriz, and Karlhans Endlich

Department of Anatomy and Cell Biology, University of Heidelberg, Heidelberg, Germany; Department of Internal Medicine, Division of Nephrology, University of Michigan, Ann Arbor, Michigan; and Department of Bacteriology and Immunology, University of Helsinki, Helsinki, Finland

Stable expression of nephrin and localization to cell-cell contacts in novel murine podocyte cell lines.

Background. Cell culture of podocytes has become an indispensable tool in the study of podocyte biology. To date, however, podocyte cell lines with stable expression of the crucial slit diaphragm protein nephrin and localization of nephrin to cell-cell contacts are not available.

Methods. Conditionally immortalized cells were grown from isolated glomeruli of mice, harboring the temperature-sensitive SV40 large T antigen. About 60 clonal cell lines were generated by limiting dilution.

Results. Among 30 Wilm's tumor (WT)-1- and podocalyxin-positive cell clones, two cell clones stably expressed nephrin as assessed by reverse transcription-polymerase chain reaction (RT-PCR), Northern and Western blotting, and immunofluorescence. In addition, expression of the following podocyte proteins was demonstrated: NEHP1, FAT, P-cadherin, podocin, CD2AP, ZO-1 (α^- isoform), Lmx1b, podoplanin, synaptopodin, cortactin, and vimentin. The nephrin-positive podocyte cell lines formed a monolayer with abundant cell-cell contacts. Transmission electron microscopy revealed formation of primitive foot process-like interdigitations and slit diaphragm-like junctions. Nephrin colocalized with F-actin at cell-cell contacts as demonstrated by immunofluorescence. Intriguingly, nephrin and actin-associated proteins (synaptopodin, CD2AP, and cortactin) were recruited to and accumulated at the entire cell margin only in confluent cells, but not in dispersed cells.

Conclusion. We present novel murine podocyte cell lines with stable expression of nephrin and abundant formation of cell-cell contacts, possessing several features of in situ podocyte cell-cell contacts. Furthermore, our data suggest that the accumulation of certain proteins in podocyte foot processes is linked to formation of cell-cell contacts.

Podocytes cover the outer aspect of the basement membrane of glomerular capillaries as a continuous layer of epithelial cells. The high glomerular filtration rate and—at the same time—the effective retention of plasma proteins is achieved by means of the highly specialized, unique cell-cell contacts of podocytes. The characteristics of podocyte cell-cell contacts are foot process interdigitation and formation of slit diaphragms. Considerable progress has been made in elucidating the molecular composition of the slit diaphragm in recent years [1–3]. The currently known slit diaphragm proteins (SDP) and slit diaphragm-associated proteins (SDAP) include nephrin [4, 5], FAT [6], P-cadherin [7], podocin [8], CD2AP [9], ZO-1 [10], and NEPH1 [11]. The dominant role of nephrin among the SDP and SDAP has been confirmed by disruption of the nephrin gene in mice [12, 13]. In these mice, the intercellular spaces between podocyte foot processes are devoid of slit diaphragms, and the mice die soon after birth by nephrotic syndrome. In addition to the discovery of SDP/SDAP, proteins that are preferentially located in podocyte foot processes have been identified (e.g., synaptopodin) [14]. Despite the increased knowledge of the molecular constituents of the slit diaphragm and foot processes, we do not yet understand the molecular arrangement and the formation of these critically important structures.

To gain further insight into the molecular make-up and the formation of the slit diaphragm and of interdigitating foot processes, suitable cell culture models will be extremely helpful. However, cell-cell contacts of the currently available podocyte cell lines share only limited characteristics with cell-cell contacts of podocytes in situ. The best characterized murine podocyte cell line was generated by Mundel et al [15]. These cells form multiple processes at low cell density, but they do not organize into a continuous epithelial layer. It was demonstrated that ZO-1, P-cadherin, and catenins localize to areas of cell-cell contact in these cells [7]. However, these cells express nephrin only at very early passages and in very low abundance [16, 17], and therefore the nephrin distribution in these cells has never been reported. On the

Key words: podocytes, nephrin, cell-cell contact.

Received for publication January 28, 2003
and in revised form May 27, 2003, and November 3, 2003
Accepted for publication February 3, 2004

other hand, two recently generated human podocyte cell lines have been reported to express nephrin [18, 19]. In both cell lines, however, nephrin is not located at cell-cell contacts [18–20].

The aim of our present work was to generate a number of conditionally immortalized murine podocyte cell clones [characterized by Wilm's tumor (WT-1) and podocalyxin expression], and to select those clones that stably express nephrin and that form a continuous epithelial layer in the differentiated state. We reasoned that these selection criteria would yield podocyte cell lines retaining features of podocyte cell-cell contacts in situ. We obtained two podocyte cell lines (PCLs) that fulfilled the selection criteria. These novel PCLs recapitulate several characteristics of cell-cell contacts of podocytes in situ, as demonstrated by expression of SDP/SDAP, by the ultrastructural properties of cell-cell contacts, and by accumulation of nephrin and actin-associated proteins at areas of cell-cell contact.

METHODS

Cell culture and generation of conditionally immortalized mouse PCLs

Glomeruli were isolated from kidneys of ImmortoMouse® mice (Charles River, St. Louis, MO, USA), carrying a temperature-sensitive mutant of the immortalizing SV40 large T antigen under control of the interferon-γ (INF-γ)-inducible H-2K^b promoter [15, 21]. The isolation of glomeruli was done by three-step sieving of renal cortices (250, 100, and 70 μm) as described earlier [22]. Isolated glomeruli were maintained in RPMI 1640 (Life Technologies, Karlsruhe, Germany) supplemented with 10% fetal bovine serum (FBS) (Boehringer Mannheim, Mannheim, Germany), 100 U/mL penicillin, 0.1 mg/mL streptomycin, and 10 U/mL mouse recombinant INF-γ (Life Technologies). The outgrowth of podocytes started between days 2 and 3. After 6 days of primary culture, glomeruli were removed and the cells were trypsinized. To propagate podocytes, cells were cultivated at 33°C in the presence of INF-γ (permissive conditions). Clonal cell lines were generated by limiting dilution of the initial pool of growing cells. To induce differentiation, podocytes were maintained at 38°C without INF-γ for at least 2 weeks (nonpermissive conditions). A higher temperature to induce differentiation as compared to that described by Mundel et al [15] was chosen, because the inactivation of the temperature-sensitive mutant of the SV40 large T antigen is enhanced at 38°C [21], and because the higher temperature matches the body temperature of the mouse (38°C to 39°C). Podocyte phenotype of differentiated cell clones was assessed by WT-1 immunofluorescence and podocalyxin reverse transcription-polymerase chain reaction (RT-PCR) [23, 24]. Cell clones being positive for WT-1 and podocalyxin were further analyzed. NIH 3T3 fibroblasts were cultured in Dulbecco's modified Eagle's medium (DMEM) (Life Technologies) supplemented with 10% FBS, 100 U/mL penicillin, and 0.1 mg/mL streptomycin.

Assessment of cell proliferation

PCL between passages 15 and 31 were seeded in 96-well plates for the 3-[4, 5]dimethylthiaozl-2,5-diphenyltetrazolium bromide (MTT) (Sigma, Deisenhofen, Germany) assay or in 6-well plates for counting. Plates were shifted to nonpermissive culture conditions (day 0). During 4 weeks, cell proliferation was assessed in regular time intervals of 2 to 3 days. In the MTT assay, MTT was added at a final concentration of 0.5 mg/mL to the wells, cells were incubated for 5 hours at 38°C, and the purple formazan crystals were solubilized in dimethyl sulfoxide (DMSO). Optical density was measured with a microplate reader (Benchmark) (Bio-Rad, Munich, Germany) at 595 nm against a reference wavelength of 655 nm. Six wells were measured for each time point in each experiment. Data are presented as means ± SEM of three experiments. The linear correlation between cell number and optical density was verified in additional experiments. In counting experiments, cells were trypsinized and counted manually in a hemocytometer. The percentage of viable cells was greater than 95%.

RNA isolation and RT-PCR

Total RNA of cultured podocytes or mouse kidneys was isolated with a mixture of guanidine thiocyanate and phenol (TRI Reagent) (Sigma) according to the manufacturer's protocol. RT was performed at 37°C for 60 minutes with 1 to 2 μg RNA. The reaction mixture contained 50 U MuLV reverse transcriptase (Applied Biosystems, Darmstadt, Germany), 10 U RNase inhibitor (Applied Biosystems), 10 mmol/L Tris-HCl (pH 8.3), 50 mmol/L KCl, 1.5 mmol/L $MgCl_2$, 10 mmol/L deoxynucleoside triphosphate (dNTP) (Sigma), and 1 μmol/L antisense oligonucleotide primer (cf., Table 1). Reaction mixes lacking RT served as negative controls. PCR was performed in the presence of 10 mmol/L Tris-HCl (pH 8.3), 50 mmol/L KCl, 1.5 mmol/L $MgCl_2$, 1 μmol/L sense oligonucleotide primer (cf. Table 1) and Taq polymerase (Eppendorf). The number of cycles ranged from 25 to 40 with 2 minutes at 94°C, $1^1/_2$ minutes at the annealing temperature, and 2 minutes at 72°C. PCR products were separated on 2% ethidium bromide-stained agarose gels, which were recorded with a digitizing video system (Intas, Göttingen, Germany). The sequence specificity of the amplicons was confirmed by size and endonuclease restriction analysis.

Northern blotting

RNA was isolated as described above. Total RNA (30 μg per lane) was resolved on 1% agarose-formaldehyde

Table 1. Primers for reverse transcription-polymerase chain reaction (RT-PCR)

Transcript	GenBank accession #	Primer pair	Product size *bp*
WT-1	NM144783	5′-GCCACCCCACTCCTTCATCA-3′ (forward) 5′-CGTGGTTGCTCTGCCCTTCT-3′ (reverse)	605
Lmx1b	NM010725	5′-GCGGCTGCATGGAGAAGATC-3′ (forward) 5′-GAGTCGTTCCCTGGCATTTG-3′ (reverse)	694
Nephrin	AF191090	5′-CCCCAACATCGACTTCACTT-3′ (forward) 5′-GGCAGGACATCCATGTAGAG-3′ (reverse)	372
NEPH1	AY017368	5′-CGTCTAATGACCTGCCAATC-3′ (forward) 5′-CCTCATTCATACTGCGACAG-3′ (reverse)	688
FAT	AF100960	5′-GTGATCGCCATCTTGAGCAC-3′ (forward) 5′-TTCCTTGGCAATCCTTGGTC-3′ (reverse)	821
P-Cadherin	X06340	5′-TGTCAACGAAGCCCCTGTGT-3′ (forward) 5′-CGGTGGAGTTGGGTGATGTC-3′ (reverse)	864
CD2AP	NM009847	5′-CGAGTTGGGGAAATCATCAG-3′ (forward) 5′-TGAGGTAGGGCCAGTCAAAG-3′ (reverse)	504
ZO-1 (α^+/α^- isoforms)	D14340	5′-TAGCACGGACAGTAGACACA-3′ (forward) 5′-ATGGAAGTTGGGGTTCATAG-3′ (reverse)	635 (α^+) 375 (α^-)
Podocalyxin	AF290209	5′-GAAAGGAGCCCTCTGGATGA-3′ (forward) 5′-GGGCTCAGGCACAAGTAGGT-3′ (reverse)	820
Podoplanin	NM010329	5′-TGGAGGGCTTAATGAATCTA-3′ (forward) 5′-GGGCTGGAATGTGTATGTAT-3′ (reverse)	799

gels and blotted onto Hybond-NX nylon membranes (Amersham Pharmacia Biotech, Buckinghamshire, UK) overnight. Probes were generated by RT-PCR as described above from mouse total kidney RNA using the following primer pairs: mouse glyceraldehyde-3-phosphate dehydrogenase (GAPDH) (GenBank accession # NM_008084), forward 5′-GTG AAG GTC GGT GTG AAC GGA TTT G-3′, reverse 5′-ACA TTG GGG GTA GGA ACA CGG AAG G-3′, 710 bp product size; mouse nephrin (GenBank accession # AF191090), forward 5′-TGC TGC CCA CGG ATG AGA CA-3′, reverse 5′-GGT CAC TGC CCG CAC TTG CT-3′, 830 bp product size; mouse CD2AP as indicated in Table 1. Probes were ^{32}P-labeled with the RadPrime DNA Labeling System (Invitrogen, Karlsruhe, Germany). Prehybridization was done in PerfectHyb Plus Hybridization Buffer (Sigma) at 65°C for 2 hours. Membranes were hybridized in 7 mL PerfectHyb Plus Hybridization Buffer containing the ^{32}P-labeled probe at 65°C overnight. Membranes were washed in 1 × standard saline citrate (SSC) containing 0.1% sodium dodecyl citrate (SDS) for 20 minutes at room temperature, and twice in 0.1 × SSC containing 0.1% SDS for 20 minutes at 65°C. Blots were exposed to x-ray films (Super RX) (Fuji, Düsseldorf, Germany) for 1 to 4 days at −80°C. Blots were stripped for 30 minutes in 0.1 × SSC containing 0.1% SDS, which had been heated to 100°C before, and stripped blots were reprobed for GAPDH expression as a loading control.

Western blotting

Podocytes were lyzed in phosphate-buffered saline (PBS) containing 2% Triton X-100, supplemented with a proteinase inhibitor cocktail (Sigma). Lysates of COS7 cells (kindly provided by Dr. M. Moeller, University of Heidelberg, Germany), which had been transiently transfected with 3xHA-tagged podocin, including or excluding the C-terminus, were employed as positive or negative control, respectively. Protein concentration was determined by the Bradford method. The lysates were heated to 100°C for 3 minutes in SDS gel-loading buffer (50 mmol/L Tris-HCl at pH 6.8, 100 mmol/L dithiothreitol, 2% SDS, 0.1% bromophenol blue, and 10% glycerol) and 30 μg protein/lane were separated on a 10% SDS polyacrylamide gel. After blotting on a polyvinylidene difluoride (PVDF) membrane (Millipore, Eschborn, Germany), membranes were blocked overnight at 4°C in blocking buffer (5% nonfat dry milk, 0.9% NaCl, 20 mmol/L Tris-HCl at pH 7.5, and 0.05% Tween). Blots were then incubated with the primary antibody (rabbit antimouse nephrin antibody directed against the 155 C-terminal amino acids [4] or rabbit antihuman/antimouse podocin antibody directed against the 17 C-terminal amino acids [25]) diluted in blocking buffer for 2 hours at room temperature, followed by rinsing with washing buffer (0.9% NaCl, 20 mmol/L Tris-HCl at pH 7.5, and 0.05% Tween). Afterwards the blot was incubated with horseradish peroxidase-labeled secondary antirabbit antibody (Sigma) for 1 hour at room temperature, washed, incubated for 1 minute in chemiluminescence solution (ECL) Amersham Pharmacia Biotech) and finally exposed to x-ray film (Hyperfilm ECL) (Amersham Pharmacia Biotech).

Immunofluorescence and microscopy

For immunofluorescence studies podocytes were cultured on type IV collagen-coated glass coverslips (Biochrom, Berlin, Germany). At room temperature cells were fixed (2% paraformaldehyde, 4% sucrose,

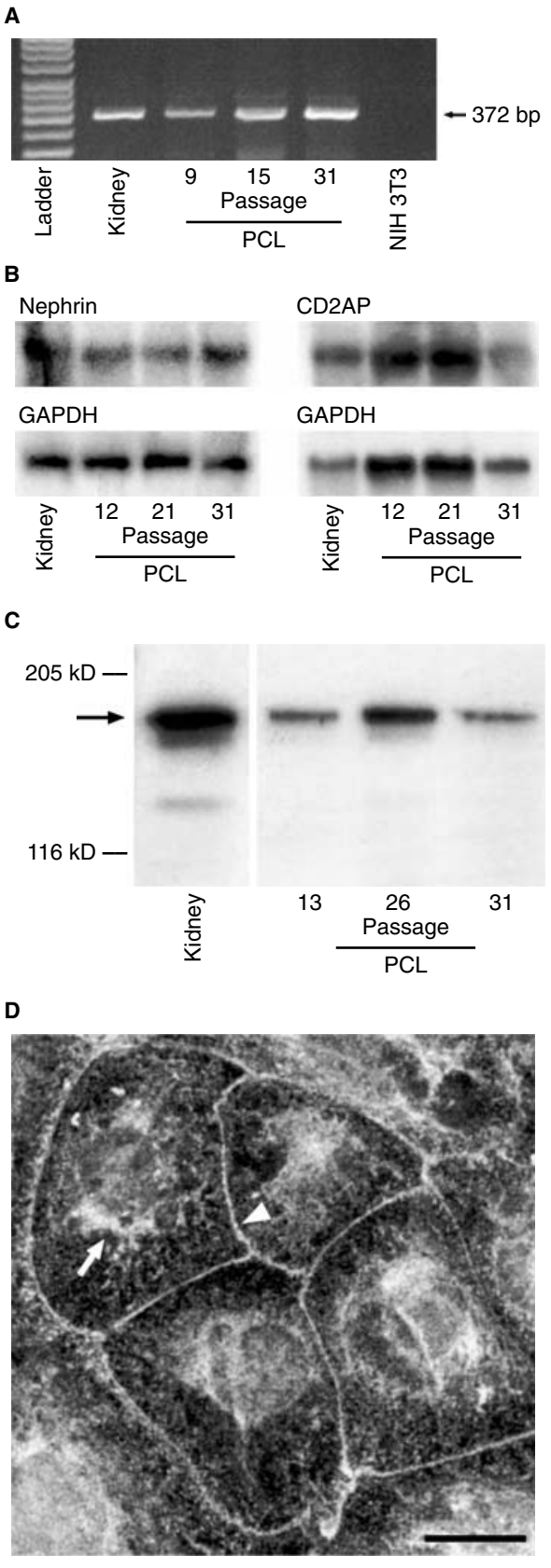

PBS) for 8 minutes, permeabilized (0.3% Triton X-100 in PBS) for 10 minutes, and blocked in blocking solution [2% FBS, 2% bovine serum albumin (BSA), 0.2% gelatine, and PBS] for 45 minutes. Primary antibodies were incubated for 60 minutes. The following antibodies were used: rabbit anti-WT-1 (C-19) (Santa Cruz Biotechnology, Santa Cruz, CA, USA), rabbit antipodocalyxin (kindly provided by Dr. M.G. Farquhar, University of California, San Diego, CA, USA), mouse antivimentin (clone VIM 13.2) (Sigma), rabbit anti-CD2AP (kindly provided by Dr. A.S. Shaw, Washington University School of Medicine, St. Louis, MO, USA) and H-290 (Santa Cruz Biotechnology), rabbit anticortactin (kindly provided by Dr. X. Zhan, American Red Cross, Rockville, MD, USA), rabbit antipodocin (kindly provided by Dr. C. Antignac, INSERM U423, Hôpital Necker-Enfants Malades, Paris, France), and mouse antisynaptopodin (Progen, Heidelberg, Germany). A polyclonal antipeptide antibody against nephrin was produced in the rabbit as described earlier [26]. A synthetic peptide covering amino acids 1039 to 1056 of the human nephrin sequence was used as the immunogen (GenBank accession # AF035835). The synthetic peptide in Freund's complete adjuvant was injected into two rabbits. After three booster inmmunizations 4 weeks apart, the respective IgG fractions were immunoaffinity-purified on CNBr-sepharose coupled to the synthetic peptide. The specificity of antisera was tested by indirect immunofluorescence and by Western blotting as well as appropriate preincubations with the immunogen. In addition, a guinea pig antinephrin antibody directed against the fibronectin domain of nephrin was utilized (Progen). Similar results were obtained with both antibodies. Antigen-antibody complexes were visualized with Cy2- or Cy3-conjugated secondary antibodies (Dianova, Hamburg, Germany). F-actin was visualized using fluorochrome-conjugated phalloidins (Molecular Probes, Eugene, OR, USA). Coverslips were washed (PBS), rinsed (H_2O), and mounted with 15% Mowiol (Calbiochem, Bad Soden, Germany), 50% glycerol, and PBS. Specimens were viewed with a confocal laser-scanning microscope (TCS-SP) (Leica Microsystems,

Fig. 1. Nephrin expression in podocyte cell line (PCL). (*A*) Ethidium bromide-stained gel of reverse transcription-polymerase chain reaction (RT-PCR) products demonstrates stable nephrin expression in PCL over different passages. (*B*) Northern blots further demonstrate stable expression of nephrin and CD2AP in PCL over different passages. (*C*) Western blotting of whole kidney and PCL lysates confirms stable nephrin expression at the protein level over different passages in PCL. (*D*) In confluent PCL cells, nephrin is located at the perinuclear region (arrow), probably corresponding to the Golgi apparatus, and at cell-cell contacts (arrow head) by immunofluorescence. For immunofluorescence PCL cells above passage 30 were used (scale bar indicates 10 μm).

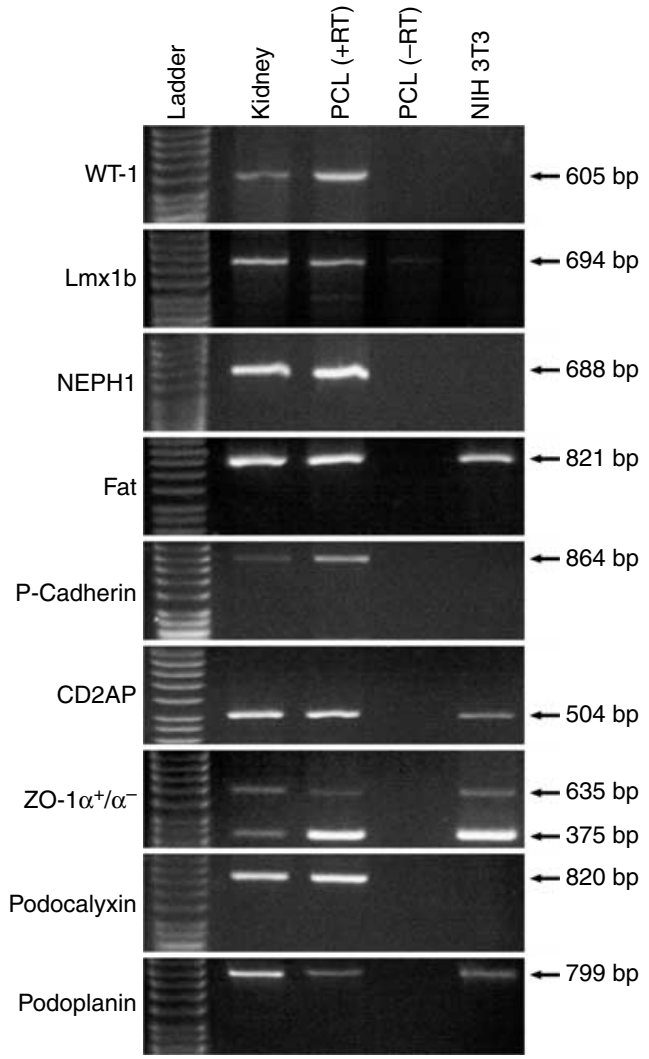

Fig. 2. Expression of slit diaphragm-associated proteins and further podocyte markers in podocyte cell line (PCL). Transcripts of podocyte-specific transcription factors [Wilm's tumor (WT-1), Lmx1b], slit diaphragm protein (SDP)/slit diaphragm-associated protein (SDAP) (NEPH1, FAT, P-cadherin, and CD2AP, α^- isoform of ZO-1), and podocyte transmembrane proteins (podocalyxin and podoplanin) were detected by reverse transcription-polymerase chain reaction (RT-PCR) in PCL. Reactions with RNA isolated from PCL were performed in the presence (+RT) and absence of reverse transcriptase (−RT). Total RNA isolated from mouse kidneys and NIH 3T3 fibroblasts served as positive and negative controls, respectively.

Mannheim, Germany). Phase contrast images were taken with a Leica IRBE microscope (Leica Microsystems) equipped with a cooled charged coupled device (CCD) camera (Photonic Science, Robertsbridge, UK) and OpenLab software (Improvision, Coventry, UK) for image acquisition.

Transmission electron microscopy

Cells were fixed in 2% glutaraldehyde with 0.2% tannin in PBS, stained in 1% OsO_4 for 30 minutes, and contrasted with 1% uranyl acetate for 30 minutes. After dehydration in alcohol, specimens were embedded in Epon 812, and 90 nm sections were cut with an ultramicrotome (Ultracut E) (Leica Microsystems). Sections were placed on Formvar-coated copper grids and examined under a transmission electron microscope (Philips EM 301).

RESULTS

Using limiting dilution we generated about 60 cell clones from the outgrowth of glomeruli which were isolated from H-2K^b-tsA58 transgenic mice carrying a temperature-sensitive variant of the SV40 large T antigen under control of the IFN-γ–inducible H-2K^b promoter [21]. Immunofluorescence staining for WT-1 and expression of podocalyxin by RT-PCR was observed in 30 cell clones, indicating that cells were of podocyte and not of parietal epithelial origin [24]. Transcripts for nephrin were detected in two of the 30 cell clones by RT-PCR. These two nephrin-expressing PCLs were characterized in detail. Since practically identical results were obtained with both PCLs, data will be presented essentially for one PCL.

PCLs could be cultured successfully over 40 passages without noting phenotypic changes. Nephrin was stably expressed in PCLs over all passages as determined by RT-PCR (Fig. 1A). In addition, stable expression of nephrin in PCLs could be demonstrated by Northern blotting using GAPDH as an internal control (Fig. 1B). Stable nephrin expression at the protein level was confirmed by Western blotting, yielding bands at about 180 kD (Fig. 1C). In confluent PCLs, nephrin was located at the perinuclear region and at cell-cell contacts as visualized by immunofluorescence (Fig. 1D). The pattern of nephrin immunoreactivity at cell-cell contacts varied from discrete dots to a continuous band, reflecting different states of confluence and junction formation (see below).

Expression of various podocyte-specific proteins, especially of SDP/SDAP, was examined by RT-PCR and immunofluorescence in PCLs. Transcripts of the podocyte transcription factors WT-1 and Lmx1b [23, 27] were detected (Fig. 2). Interestingly, among the 30 cell clones that showed nuclear immunoreactivity for WT-1, the two nephrin-positive cell clones expressed WT-1 at the highest level as observed by RT-PCR. Besides nephrin, transcripts of the SDP/SDAP NEPH1, FAT, P-cadherin, CD2AP, and ZO-1 were present in PCLs (Fig. 2). Concerning ZO-1, the podocyte-specific α^- splice variant [28] was the almost exclusively expressed isoform. Finally, transcripts of the podocyte transmembrane proteins podocalyxin and podoplanin [29, 30], which are also expressed in other cell types, were detected in PCLs. In kidney RNA, PCR products could be amplified for all transcripts tested (Fig. 2). Northern blotting showed stable expression of CD2AP in PCLs over different passages (Fig. 1B). Expression of podocin could be

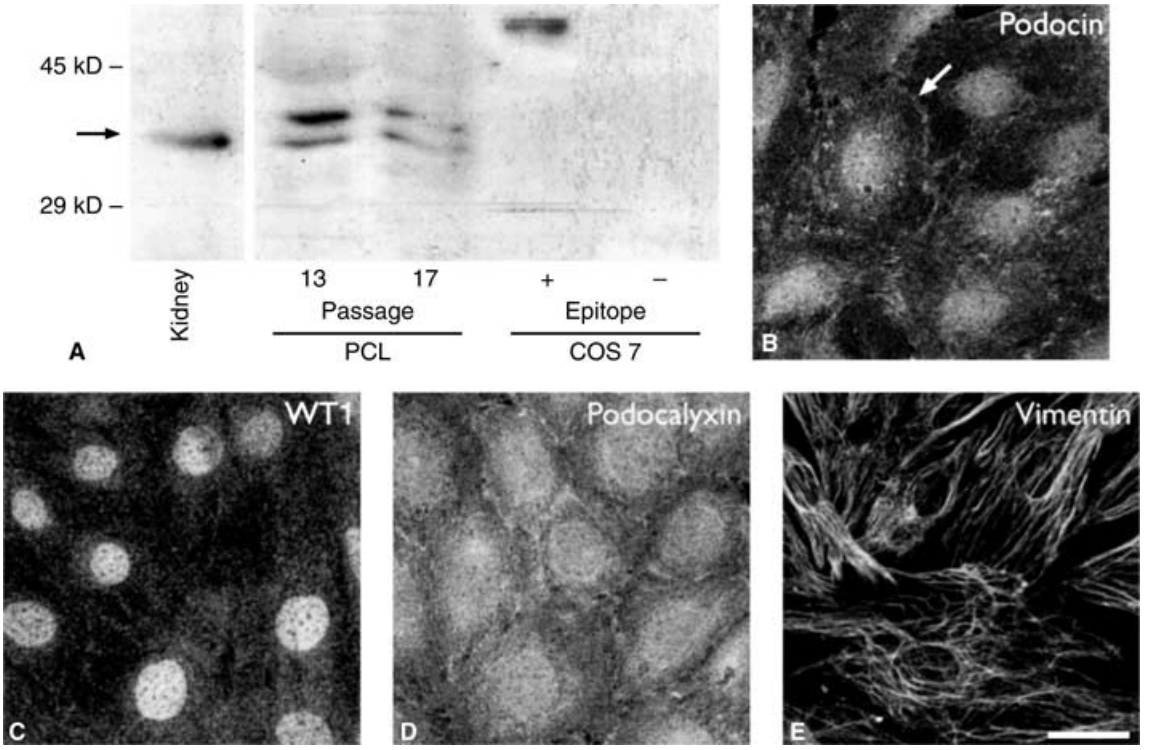

Fig. 3. Expression of podocin and subcellular distribution of podocyte markers in podocyte cell line (PCL). (*A*) Podocin expression was detected in whole kidney and PCL lysates by Western blotting. Lysates of COS7 cells, expressing 3xHA-tagged podocin with or without epitope, served as controls. (*B*) Podocin immunoreactivity localizes to the membrane and to areas of cell-cell contact in PCL (arrow). (*C*) PCL show nuclear staining for Wilm's tumor (WT-1). (*D*) Diffuse membrane staining for podocalyxin. (*E*) Filamentous staining for vimentin (scale bar indicates 20 μm).

demonstrated at the protein level by Western blotting (Fig. 3A) and by immunofluorescence (Fig. 3B). In Western blots, bands around 39 to 40 kD were detected for podocin in agreement with previous results [25]. Podocin assumed a membranous distribution in PCLs accumulating at areas of cell-cell contact (Fig. 3B, arrow). Protein expression and localization of WT-1, podocalyxin, and the intermediate filament protein vimentin were visualized in PCLs by immunofluorescence (Fig. 3C to E). In addition, PCLs stained positively using antibodies against the actin-associated proteins CD2AP, cortactin, and synaptopodin (see Figs. 7 and 8), whose cellular distributions are described below in detail.

When PCL cells were seeded at non-confluent density, cells possessed long and short processes (Fig. 4A, arrows), resembling the arborized phenotype of conditionally immortalized podocytes generated by Mundel et al [15]. At confluence, PCLs formed a monolayer with only a few gaps between cells (Fig. 4B). When PCL cells were shifted from permissive to nonpermissive culture conditions, proliferation slowed down progressively with a population doubling time of 5.0 ± 0.7 days in the first week and 10.9 ± 1.2 days in the second week ($N = 3$). Proliferation ceased in the third and fourth week under nonpermissive conditions (Fig. 4C) as measured by the MTT assay. Similar results were obtained in cell counting experiments (data not shown).

In view of the expression of nephrin and all other SDPs/SDAPs in PCLs, we examined the ultrastructure of cell-cell contacts in confluent PCLs by transmission electron microscopy. Electron microscopy of vertical and horizontal cell sections revealed that cell-cell contacts of PCLs share characteristics with those observed in podocytes in situ (Fig. 5). PCL cells frequently possessed interlacing finger-like processes of about 150 nm width (Fig. 5, arrows). These processes formed large areas of contact with a regular spacing of 30 to 40 nm and with some electron-dense material in the intercellular space (Fig. 5, arrow heads), being reminiscent of foot process interdigitation in situ [31], however, in a very rudimentary and incomplete fashion. Tight junctions were not observed between PCL cells.

In differentiated PCL cells, the nephrin distribution was altered upon the presence of cell-cell contacts (Fig. 6A to D). Dispersed cells, which possessed no or very few cell-cell contacts, showed prominent intracellular nephrin staining (Fig. 6A). Nephrin localized to the perinuclear region and was distributed in a pattern reminiscent of focal contacts (Fig. 6A, arrow), as described by Saleem et al [19] in a human podocyte cell line.

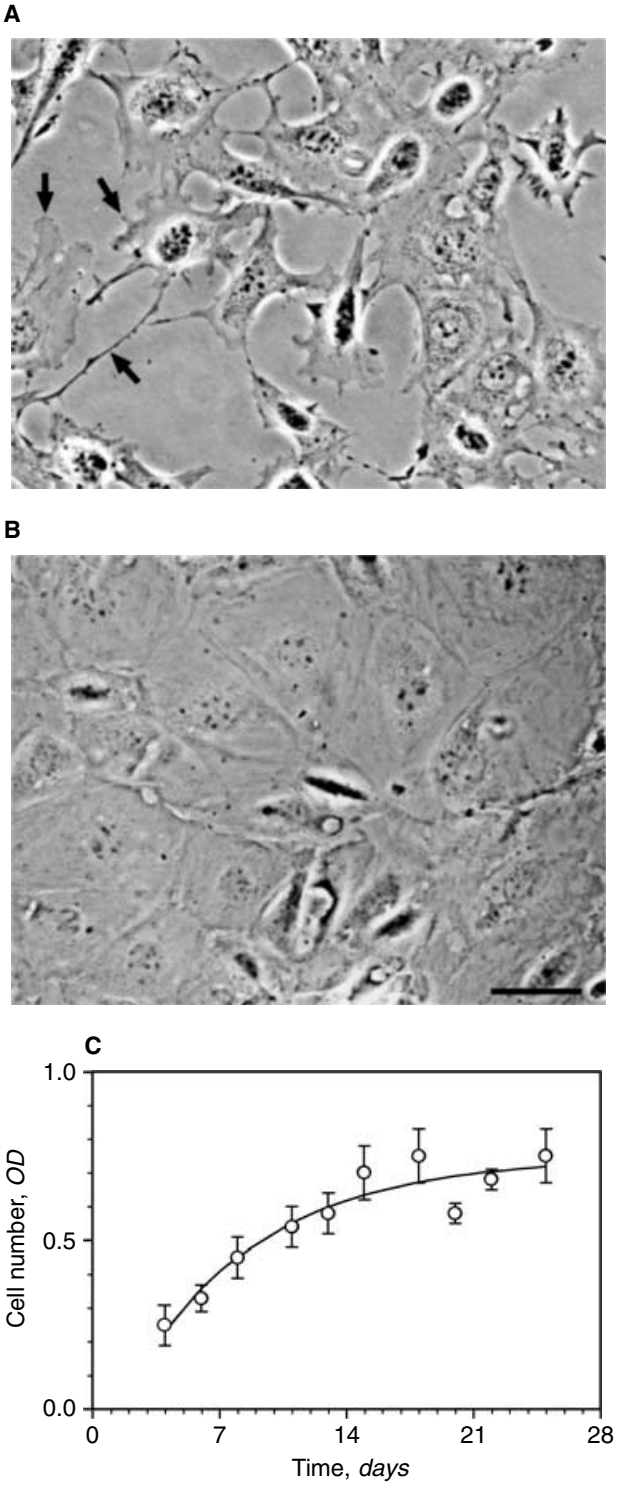

Fig. 4. Morphology and proliferation of podocyte cell line (PCL). Phase-contrast images of PCL at nonconfluent (*A*) and confluent (*B*) cell density. Nonconfluent PCL cells possess multiple processes (arrows). When PCL are shifted to non-permissive culture conditions (day 0), cell number reaches a plateau after 2 weeks (*C*). Data are means ± SEM of three experiments (scale bar indicates 50 μm).

Subconfluent PCL cells with an increased cell-cell contact area still showed the focal adhesion-like pattern of nephrin staining (Fig. 6B, arrow), but also demonstrated accumulation of nephrin in areas of cell-cell contact (Fig. 6B, arrow heads). In confluent PCL cells (Fig. 6C and D), nephrin was present predominantly along cell-cell contacts in a punctate pattern (Fig. 6C, arrow head). A fraction of confluent PCL cells displayed even stronger immunoreactivity for nephrin at cell-cell contacts, staining as continuous bands (Fig. 6D). Intracellular staining for nephrin was weak in confluent cells. Nephrin completely colocalized with F-actin at areas of cell-cell contact in confluent PCL cells (Fig. 6E to G).

Podocytes in situ are characterized by cytoskeletal compartmentalization (i.e., F-actin and several actin-associated proteins are concentrated in foot processes [32]). Among the actin-associated proteins with preferential localization in foot processes are synaptopodin [14], CD2AP [16, 33], and cortactin [2] [abstract; Besse-Eschmann V, et al, *J Am Soc Nephrol*, 13: 530A, 2002]. Immunofluorescence staining revealed that CD2AP, cortactin, and synaptopodin were concentrated at areas of cell-cell contact in confluent PCL cells (Fig. 7A to C, arrows). At areas of cell-cell contact, CD2AP, cortactin, and synaptopodin colocalized with F-actin (Fig. 7G to L). While CD2AP and cortactin colocalized with F-actin in a rather continuous, ruffle-like band along the cell border (Fig. 7J and K), synaptopodin was predominantly located at sites enriched with F-actin (Fig. 7L). In dispersed PCL cells, CD2AP, cortactin, and synaptopodin were largely absent from cell margins (Fig. 8A to C). CD2AP and cortactin staining in dispersed cells was restricted to the edge of a few processes (Fig. 8A and B, arrows); the remaining areas of the cell margin were devoid of both proteins (Fig. 8A and B, arrow heads). Synaptopodin was essentially confined to stress fibers in nonconfluent cells (Fig. 8C, arrows). A further indication, that redistribution of CD2AP, cortactin, and synaptopodin to areas of cell-cell contact occurred in a contact-dependent fashion, was obtained in confluent PCL cells where cell-free spaces were encountered occasionally. CD2AP, cortactin, and synaptopodin were enriched at areas of cell-cell contact (Fig. 8D to F, arrows), whereas cell margins without neighbors demonstrated only weak staining for the three proteins (Fig. 8D to F, arrow heads).

DISCUSSION

We have generated PCLs in which we could demonstrate expression of 14 podocyte proteins (WT-1, Lmx1b, nephrin, NEPH1, FAT, P-cadherin, podocin, CD2AP, ZO-1, podocalyxin, podoplanin, vimentin, cortactin, and synaptopodin). The novel murine PCLs represent a major advance in podocyte culture because of two unique

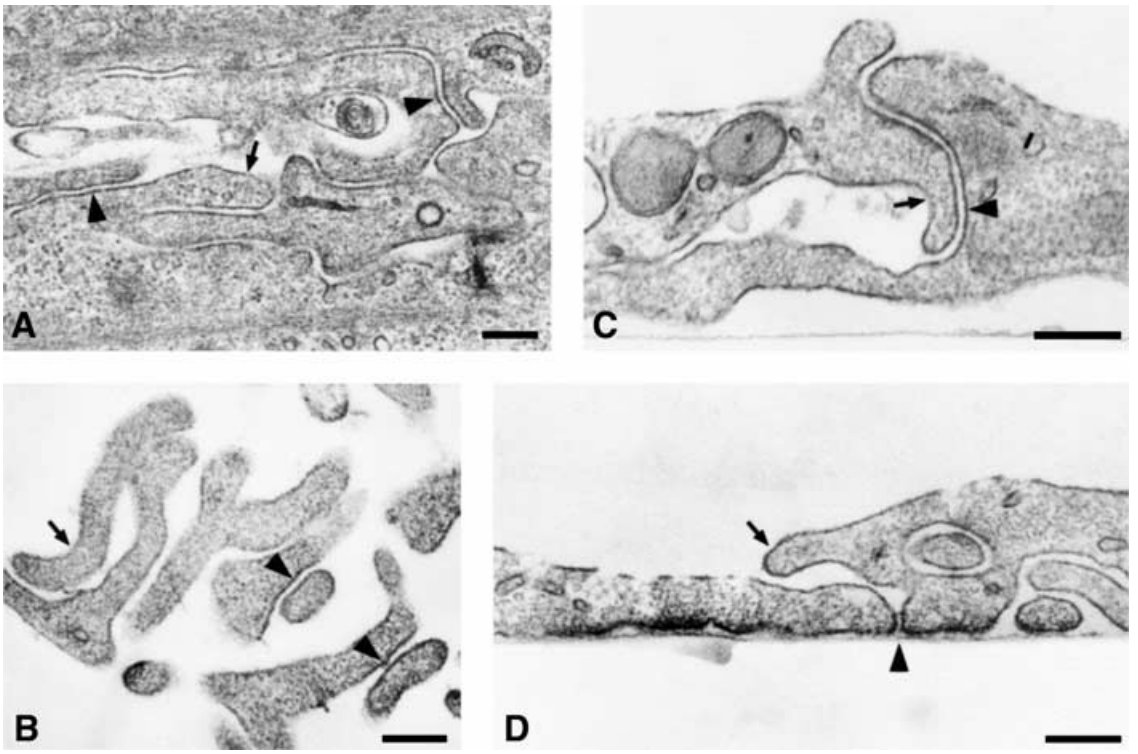

Fig. 5. Ultrastructure of cell-cell contacts in podocyte cell ine (PCL). Areas of cell-cell contact were examined in horizontal (*A* and *B*) and vertical (*C* and *D*) sections through confluent PCL cells by electron microscopy. Cell borders are characterized by interlacing finger-like processes (arrows). Cell-cell contacts frequently show a regular spacing of 30 to 40 nm with electron-dense material in-between (arrow heads) (scale bars indicate 200 nm).

features. First, the novel PCLs are the only murine podocyte cell lines with stable nephrin expression that have been generated so far. Second, the novel PCLs is the only podocyte culture system in which nephrin localizes to cell-cell contacts. Though nephrin expression has been reported in two other cell lines of podocyte origin to date, nephrin does not localize to cell-cell contacts in these human cell lines [18–20]. In these human cell lines, nephrin shows either diffuse membrane staining [18] or localizes to focal adhesion-like sites [19, 20]. This distribution of nephrin to sites reminiscent of focal adhesions can also be observed in our novel PCL cells, but only in a nonconfluent state (cf. Fig. 6). Obviously, expression of nephrin per se is not sufficient to result in localization of nephrin at cell-cell contacts. Possibly, the nephrin-expressing human cell lines lack some nephrin-interacting proteins needed to direct and/or to stabilize nephrin at cell-cell contacts. Given the critical importance of nephrin for the formation of slit diaphragms [12, 13, 34], localization of nephrin at cell-cell contacts in our novel PCLs suggests that at least some questions concerning the molecular biology of podocyte cell-cell contacts can now be addressed in vitro.

In situ, the actin-associated proteins CD2AP, cortactin, and synaptopodin are highly concentrated in podocyte foot processes [2, 14, 16, 33] [abstract; Besse-Eschmann V, et al, *J Am Soc Nephrol*, 13: 530A, 2002]. Similar to the redistribution of nephrin, we documented an enrichment of CD2AP, cortactin, and synaptopodin at areas of cell-cell contact in PCLs in a cell contact-dependent manner. CD2AP was discovered due to its ability to cluster CD2 at the immunologic synapse [35]. Later, CD2AP was shown to interact also with nephrin [9]. Two domains of CD2AP have been described to mediate nephrin-binding, a novel C-terminal domain as demonstrated in transfected HeLa cells [16], and the third SH3 domain as determined in the M1 collecting duct cell line [36]. Thus, CD2AP could accumulate at cell-cell contacts in PCLs because of its ability to cluster nephrin. On the other hand, CD2AP is not only observed in podocyte foot processes in vicinity to the slit diaphragm [16, 33], but also in other cytosolic areas [33]. The cytosolic localization may point to another possible function of CD2AP, being the regulation of actin nucleation. In this respect, we have localized CD2AP as well as cortactin, which is known to be able to activate actin nucleation [37], to small actin spots in cultured podocytes [33]. These small actin spots are likely to represent sites of highly dynamic actin turnover [38, 39]. Localization of CD2AP to one end of actin tails in ARF6 overexpressing cells provides further evidence that CD2AP might be involved in dynamic actin processes [40]. Thus accumulation of CD2AP and

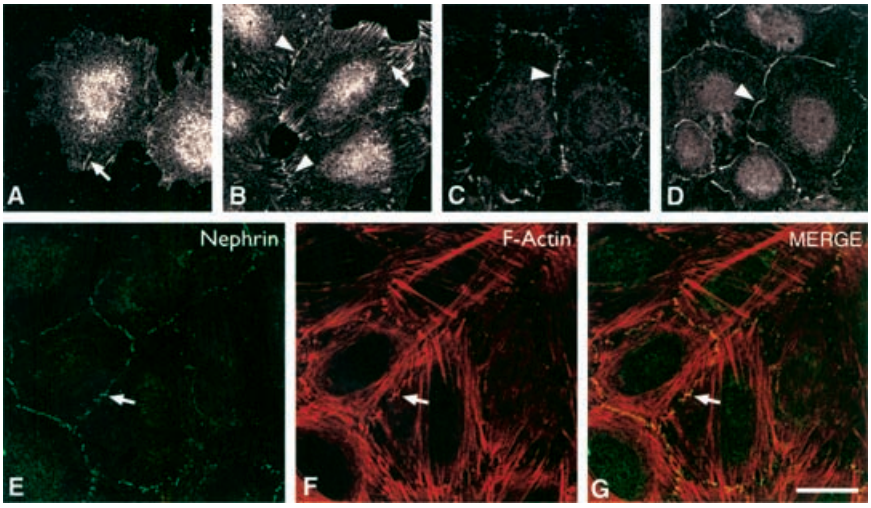

Fig. 6. Redistribution of nephrin upon cell contact in podocyte cell line (PCL). In dispersed cells with rare cell-cell contacts (*A*) and also in subconfluent cells (*B*), nephrin is concentrated in the perinuclear region and at focal adhesion-like sites (arrows). If cells possess larger areas of cell-cell contact (B) and form a continuous monolayer (*C* and *D*), nephrin is redistributed to areas of cell-cell contact (arrow heads). In most confluent cells, nephrin is concentrated in dots at cell-cell contacts (B and C) and, in some cells, continuous bands of nephrin staining are visible (D). Nephrin (*E*) colocalizes with F-actin (*F*) at areas of cell-cell contact in confluent cells (orange to yellow color in the merged image (*G*) (scale bar indicates 20 μm).

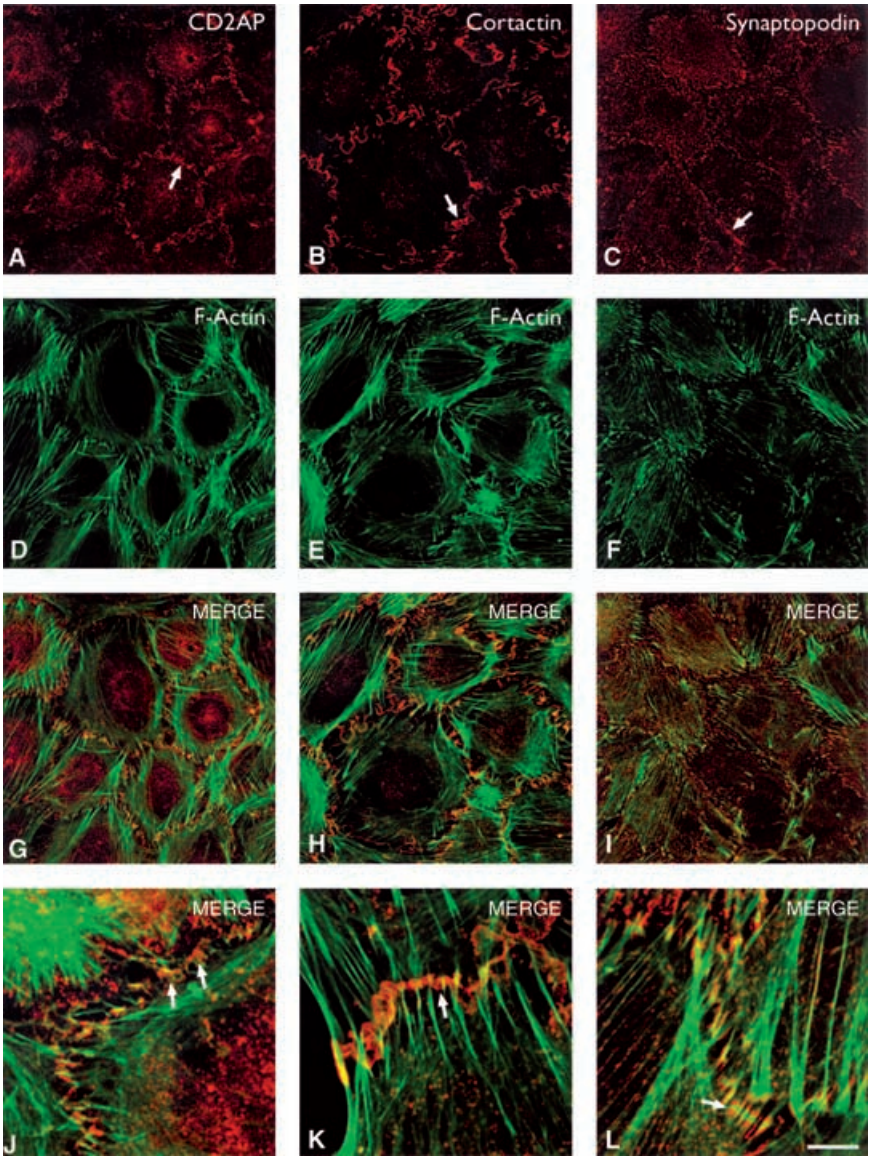

Fig. 7. Localization of actin-associated proteins in podocyte cell line (PCL). The actin-associated proteins CD2AP (left column), cortactin (middle column), and synaptopodin (right column) accumulate at areas of cell-cell contact in confluent cells (*A* to *C*, arrows). Double staining for F-actin (*D* to *F*) demonstrates that CD2AP, cortactin, and synaptopodin colocalize with F-actin along the cell borders [orange to yellow color in merged images (*G* to *I*)]. At higher magnification, concentration of synaptopodin in dense F-actin structures at the cell border is visible (I, arrow). In colocalization with F-actin, the staining pattern for CD2AP and cortactin is more continuous, and is not restricted to dense F-actin structures (*J* and *K*, arrows) [scale bar indicates 20 μm (A to I) and 5 μm (J to *L*), respectively].

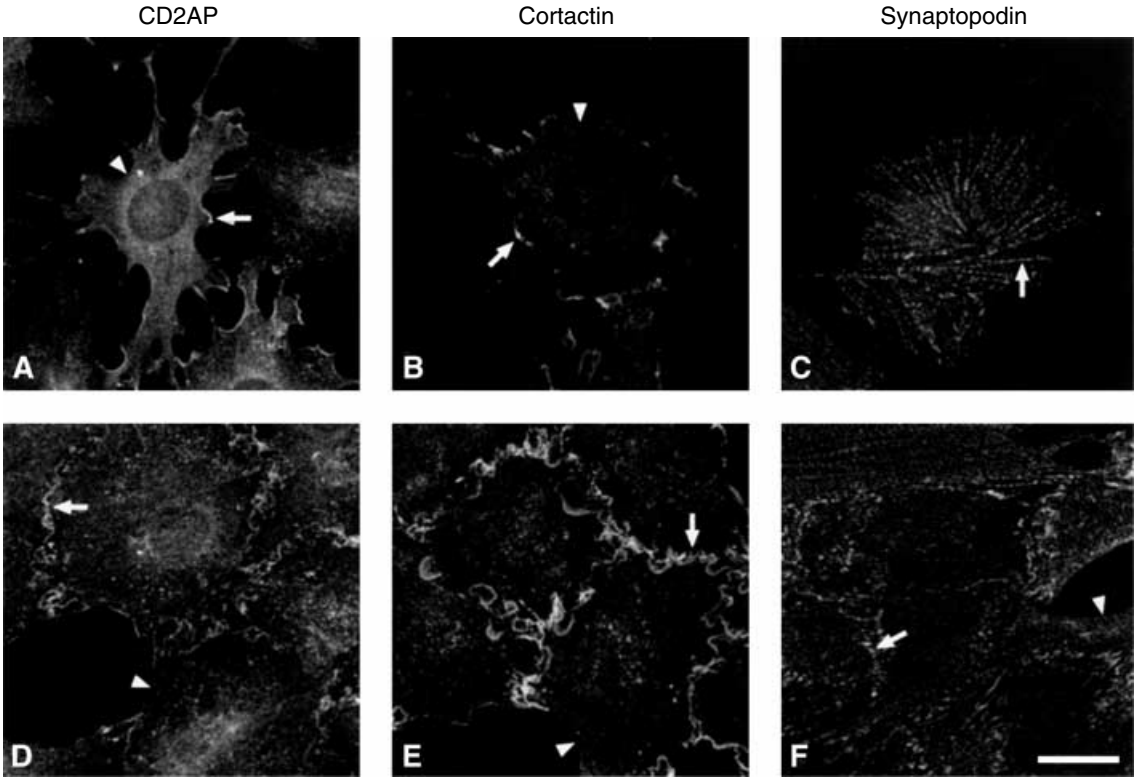

Fig. 8. Redistribution of actin-associated proteins upon cell contact in podocyte cell line (PCL). In dispersed cells, CD2AP (left column) and cortactin (middle column) are enriched at some protrusions (*A* and *B*, arrows), while large areas of cell margins remain unstained (A and B, arrow heads). Synaptopodin (right column) localizes to stress fibers in dispersed cells (*C*, arrow). In confluent cells, CD2AP, cortactin, and synaptopodin accumulate at areas of cell-cell contact (*D* to *F*, arrows), while accumulation is not observed at cell margins, which line cell-free spaces (D to F, arrow heads) (scale bar indicates 20 μm).

cortactin at areas of cell-cell contacts in PCLs could indicate contact-dependent activation of actin nucleation with recruitment of actin nucleating proteins or, alternatively, immobilization of actin nucleating proteins in cell protrusions upon contact. Interestingly, besides activating actin nucleation, cortactin has been shown to stabilize newly formed F-actin branches [41]. Whether areas of cell-cell contact in PCLs and in podocytes in situ are characterized by stable actin filaments or by dynamic actin turnover will be important to determine, since pathologic alterations of podocyte cell-cell contacts depend on the reorganization of the actin cytoskeleton [42].

Synaptopodin is an actin-bundling protein that is mainly located in stress fibers in cultured podocytes, in contrast to podocytes in situ where synaptopodin is almost exclusively found in foot processes [14]. In the PCLs presented, synaptopodin is redistributed from stress fibers to dense F-actin structures at areas of cell-cell contact. The mechanism by which synaptopodin is recruited to areas of cell-cell contact is unknown. Recently, it has been shown that synaptopodin binds to the membrane-associated guanylate kinase MAGI-1 [43]. Since MAGI-1 associates with megalin in podocytes [44], interaction of synaptopodin with MAGI-1 and other proteins might be responsible for synaptopodin targeting to areas of cell-cell contact. Whether synaptopodin, in addition to its actin-bundling activity, stimulates actin nucleation and polymerization as reported for the homologues protein fesselin [45] remains to be determined.

CONCLUSION

We present novel PCLs recapitulating characteristics of podocyte cell-cell contacts in situ. These cell lines will be of great use to study aspects of the molecular arrangement and formation of podocyte cell-cell contacts. Furthermore, our results suggest that formation of cell-cell contacts and accumulation of nephrin and actin-associated proteins in foot processes are interconnected events.

ACKNOWLEDGMENTS

We thank Claudia Kocksch for skilled and committed technical assistance, Hiltraud Hosser for expert electron microscopy imaging, Ingrid Ertl for photography, and Rolf Nonnenmacher for excellent graphic work. This study was supported by grants of the Medical Faculty of the University of Heidelberg (grant 313/2000) and the German Research Foundation (DFG, grant En 329/7–1) to K.E.

Reprint requests to Dr. Karlhans Endlich, Institut für Anatomie und Zellbiologie I, Universität Heidelberg, INF 307, D-69120 Heidelberg, Germany.
E-mail karlhans.endlich@urz.uni-heidelberg.de

REFERENCES

1. Endlich K, Kriz W, Witzgall R: Update in podocyte biology. *Curr Opin Nephrol Hypertens* 10:331–340, 2001
2. Kerjaschki D: Caught flat-footed: podocyte damage and the molecular bases of focal glomerulosclerosis. *J Clin Invest* 108:1583–1587, 2001
3. Pavenstädt H, Kriz W, Kretzler M: Cell biology of the glomerular podocyte. *Physiol Rev* 83:253–307, 2003
4. Holzman LB, St. John PL, Kovari IA, *et al*: Nephrin localizes to the slit pore of the glomerular epithelial cell. *Kidney Int* 56:1481–1491, 1999
5. Kestila M, Lenkkeri U, Mannikko M, *et al*: Positionally cloned gene for a novel glomerular protein—nephrin—is mutated in congenital nephrotic syndrome. *Mol Cell* 1:575–582, 1998
6. Inoue T, Yaoita E, Kurihara H, *et al*: FAT is a component of glomerular slit diaphragms. *Kidney Int* 59:1003–1012, 2001
7. Reiser J, Kriz W, Kretzler M, Mundel P: The glomerular slit diaphragm is a modified adherens junction. *J Am Soc Nephrol* 11:1–8, 2000
8. Boute N, Gribouval O, Roselli S, *et al*: NPHS2, encoding the glomerular protein podocin, is mutated in autosomal recessive steroid-resistant nephrotic syndrome. *Nat Genet* 24:349–354, 2000
9. Shih NY, Li J, Karpitskii V, *et al*: Congenital nephrotic syndrome in mice lacking CD2-associated protein. *Science* 286:312–315, 1999
10. Schnabel E, Anderson JM, Farquhar MG: The tight junction protein ZO-1 is concentrated along slit diaphragms of the glomerular epithelium. *J Cell Biol* 111:1255–1263, 1990
11. Barletta GM, Kovari IA, Verma RK, *et al*: Nephrin and Neph1 co-localize at the podocyte foot process intercellular junction and form cis hetero-oligomers. *J Biol Chem* 278:19266–19271, 2003
12. Putaala H, Soininen R, Kilpelainen P, *et al*: The murine nephrin gene is specifically expressed in kidney, brain and pancreas: inactivation of the gene leads to massive proteinuria and neonatal death. *Hum Mol Genet* 10:1–8, 2001
13. Rantanen M, Palmen T, Patari A, *et al*: Nephrin TRAP mice lack slit diaphragms and show fibrotic glomeruli and cystic tubular lesions. *J Am Soc Nephrol* 13:1586–1594, 2002
14. Mundel P, Heid HW, Mundel TM, *et al*: Synaptopodin: an actin-associated protein in telencephalic dendrites and renal podocytes. *J Cell Biol* 139:193–204, 1997
15. Mundel P, Reiser J, Borja AZ, *et al*: Rearrangements of the cytoskeleton and cell contacts induce process formation during differentiation of conditionally immortalized mouse podocyte cell lines. *Exp Cell Res* 236:248–258, 1997
16. Shih NY, Li J, Cotran R, *et al*: CD2AP localizes to the slit diaphragm and binds to nephrin via a novel C-terminal domain. *Am J Pathol* 159:2303–2308, 2001
17. Yan K, Khoshnoodi J, Ruotsalainen V, Tryggvason K: N-linked glycosylation is critical for the plasma membrane localization of nephrin. *J Am Soc Nephrol* 13:1385–1389, 2002
18. Doublier S, Routsalainen V, Salvidio G, *et al*: Nephrin redistribution on podocytes is a potential mechanism for proteinuria in patients with primary acquired nephrotic syndrome. *Am J Pathol* 158:1723–1731, 2001
19. Saleem MA, O'Hare MJ, Reiser J, *et al*: A conditionally immortalized human podocyte cell line demonstrating nephrin and podocin expression. *J Am Soc Nephrol* 13:630–638, 2002
20. Saleem MA, Ni L, Witherden I, *et al*: Co-localization of nephrin, podocin, and the actin cytoskeleton: evidence for a role in podocyte foot process formation. *Am J Pathol* 161:1459–1466, 2002
21. Jat PS, Noble MD, Ataliotis P, *et al*: Direct derivation of conditionally immortal cell lines from an H-2K^b-tsA58 transgenic mouse. *Proc Natl Acad Sci USA* 88:5096–5100, 1991
22. Endlich N, Kress KR, Reiser J, *et al*: Podocytes respond to mechanical stress in vitro. *J Am Soc Nephrol* 12:413–422, 2001
23. Mundlos S, Pelletier J, Darveau A, *et al*: Nuclear localiziation of the protein encoded by the Wilm's tumor gene WT1 in embryonic and adult tissues. *Development* 119:1329–1341, 1993
24. Yaoita E, Kurihara H, Sakai T, *et al*: Phenotypic modulation of parietal epithelial cells of Bowman's capsule in culture. *Cell Tissue Res* 304:339–349, 2001
25. Moeller MJ, Sanden SK, Soofi A, *et al*: Two gene fragments that direct podocyte-specific expression in transgenic mice. *J Am Soc Nephrol* 13:1561–1567, 2002
26. Ahola H, Wang SX, Luimula P, *et al*: Cloning and expression of the rat nephrin homolog. *Am J Pathol* 155:907–913, 1999
27. Chen H, Lun Y, Ovchinnikov D, *et al*: Limb and kidney defects in Lmx1b mutant mice suggest an involvement of LMX1B in human nail patella syndrome. *Nat Genet* 19:51–55, 1998
28. Kurihara H, Anderson JM, Farquhar MG: Diversity among tight junctions in rat kidney: Glomerular slit diaphragms and endothelial junctions express only one isoform of the tight junction protein ZO-1. *Proc Natl Acad Sci USA* 89:7075–7079, 1992
29. Breiteneder-Geleff S, Matsui K, Soleiman A, *et al*: Podoplanin, novel 43-kd membrane protein of glomerular epithelial cells, is down-regulated in puromycin nephrosis. *Am J Pathol* 151:1141–1152, 1997
30. Kerjaschki D, Sharkey DJ, Farquhar MG: Identification and characterization of podocalyxin—The major sialoprotein of the renal glomerular epithelial cell. *J Cell Biol* 98:1591–1596, 1984
31. Rodewald R, Karnovsky MJ: Porous substructure of the glomerular slit diaphragm in the rat and mouse. *J Cell Biol* 60:423–433, 1972
32. Mundel P, Kriz W: Structure and function of podocytes: an update. *Anat Embryol (Berlin)* 192:385–397, 1995
33. Welsch T, Endlich N, Kriz W, Endlich K: CD2AP and p130Cas localize to different F-actin structures in podocytes. *Am J Physiol Renal Physiol* 281:F769–F777, 2001
34. Tryggvason K, Wartiovaara J: Molecular basis of glomerular permselectivity. *Curr Opin Nephrol Hypertens* 10:543–549, 2001
35. Dustin ML, Olszowy MW, Holdorf AD, *et al*: A novel adaptor protein orchestrates receptor patterning and cytoskeletal polarity in T-cell contacts. *Cell* 94:667–677, 1998
36. Palmen T, Lehtonen S, Ora A, *et al*: Interaction of endogenous nephrin and CD2-associated protein in mouse epithelial M-1 cell line. *J Am Soc Nephrol* 13:1766–1772, 2002
37. Uruno T, Liu J, Zhang P, *et al*: Activation of Arp2/3 complex-mediated actin polymerization by cortactin. *Nat Cell Biol* 3:259–266, 2001
38. Schafer DA, Welch MD, Machesky LM, *et al*: Visualization and molecular analysis of actin assembly in living cells. *J Cell Biol* 143:1919–1930, 1998
39. Kaksonen M, Peng HB, Rauvala H: Association of cortactin with dynamic actin in lamellipodia and on endosomal vesicles. *J Cell Sci* 113:4421–4426, 2000
40. Schafer DA, D'Souza-Schorey C, Cooper JA: Actin assembly at membranes controlled by ARF6. *Traffic* 1:896–907, 2000
41. Weaver AM, Karginov AV, Kinley AW, *et al*: Cortactin promotes and stabilizes Arp2/3-induced actin filament network formation. *Curr Biol* 11:370–374, 2001
42. Kerjaschki D: Polycation-induced dislocation of slit diaphragms and formation of cell junctions in rat kidney glomeruli: the effects of low temperature, divalent cations, colchicine, and cytochalasin B. *Lab Invest* 39:430–440, 1978
43. Patrie KM, Drescher AJ, Welihinda A, *et al*: Interaction of two actin-binding proteins, synaptopodin and alpha-actinin-4, with the tight junction protein MAGI-1. *J Biol Chem* 277:30183–30190, 2002
44. Patrie KM, Drescher AJ, Goyal M, *et al*: The membrane-associated guanylate kinase protein MAGI-1 binds megalin and is present in glomerular podocytes. *J Am Soc Nephrol* 12:667–677, 2001
45. Beall B, Chalovich JM: Fesselin, a synaptopodin-like protein, stimulates actin nucleation and polymerization. *Biochemistry* 40:14252–14259, 2001